catalysts

Supplementary Figures and Tables

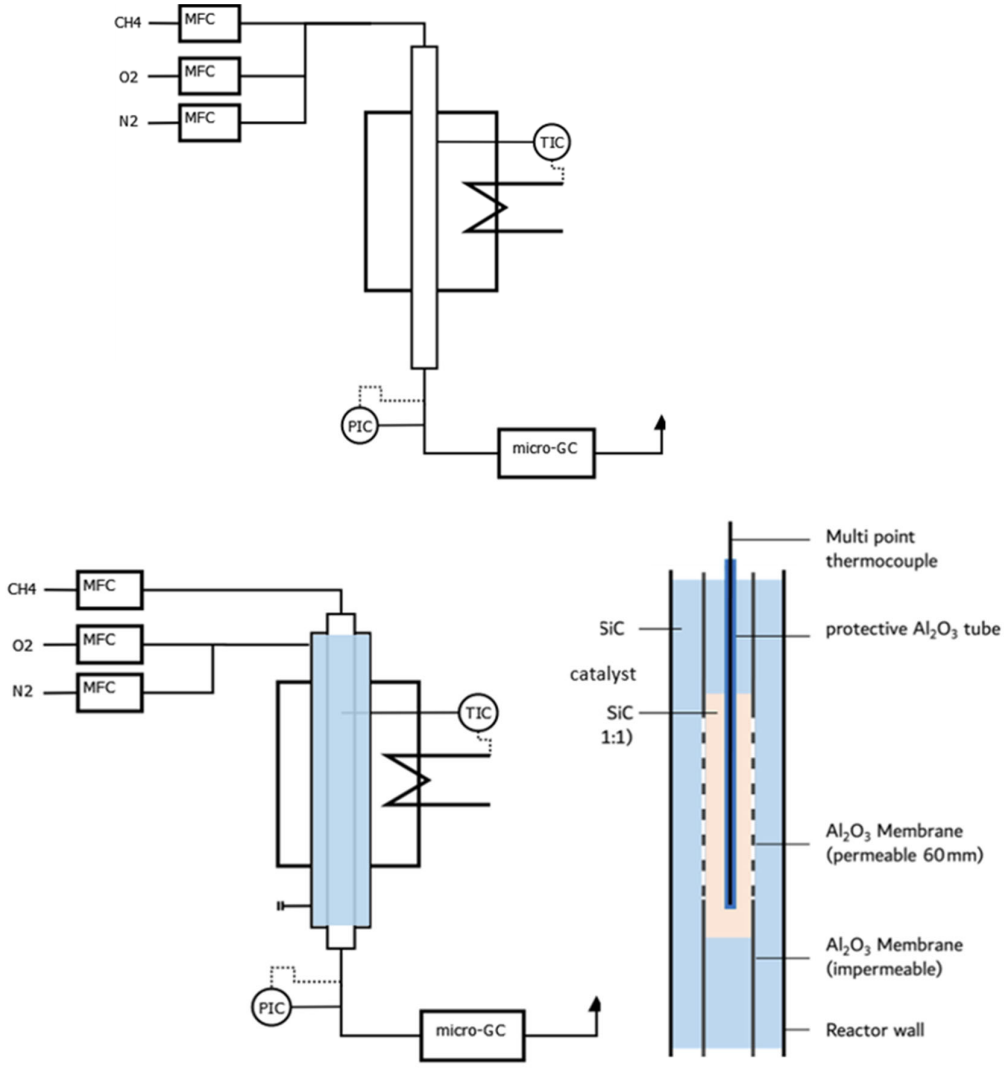

Figure S1. Schematic illustration of TUB miniplant experimental setup for Fixed Bed Reactor (top) and Membrane Fixed Bed Reactor (bottom)

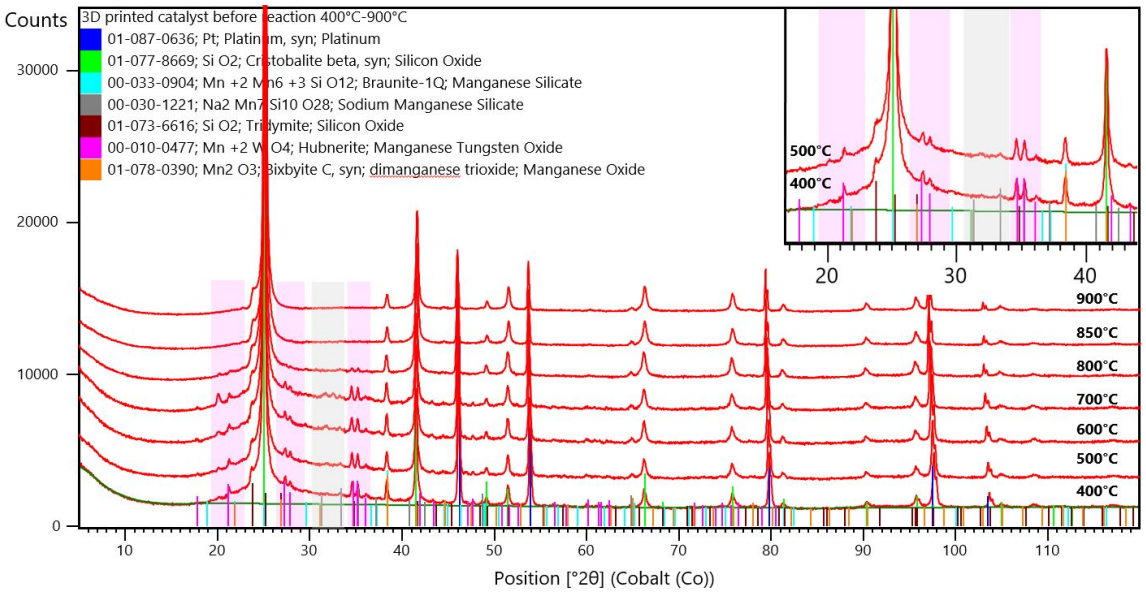

Figure S2. XRD patterns and identified phases during a temperature ramp from 400 ˚C to 900 °C and back at room temperature. The insert shows a zoomed in region of 2θ of 20-40° with the identified reflections with no pattern changes with temperature at 400 °C and 500 °C

	space group		a	b	c	RT	400°C	500°C	600°C	700°C	800°C	850°C	900°C	1000°C	RT
			Å	Å	Å										
SiO2-cristobalite	tetragonal	alfa-low	4.9694		6.9256										
SiO2-cristobalite	tetragonal	alfa-high	4.9829		6.9633										
SiO2-cristobalite	orthorombic	beta	7.1315	7.1315	7.1315										
SiO2-cristobalite	cubic	beta	7.1471												
SiO2-tridymite-O	orthorombic		17.0859	9.9313	16.304										
SiO2-tridymite	orthorombic		8.743	5.046	8.254										
SiO2-tridymite	hexagonal		5.03		8.22										
Mn2O3	orthorombic		9.4078	9.4488	9.3739										
Mn2O3	cubic	Bixbyite	9.43												
MnWO4	monoclinic		4.762	5.66	4.9507										
Mn2WO4	monoclinic	Hubnerite	4.83	5.77	4.98										
Na2WO4	cubic		9.13												
Mn3O4	cubic		8.7												
Mn7SiO12	tetragonal	Braunite	9.425		18.699										

Table S1. Summary of XRD results and identified phases during a temperature ramp from room temperature/400 ˚C to 1000 °C and back at room temperature. The table includes respective space groups and lattice parameters at different temperatures obtained from Rietveld analysis.

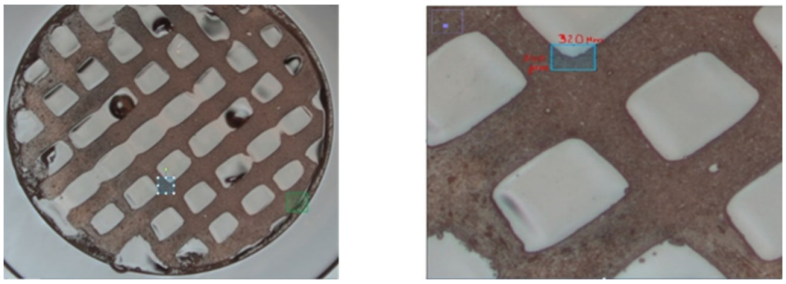

Figure S3. Optical images of a cross section of a 3D printed Mn-Na-W/SiO_2 catalyst embedded in epoxy resin. The blue rectangle indicates a region of interest presented in greater detail in Figure S6.

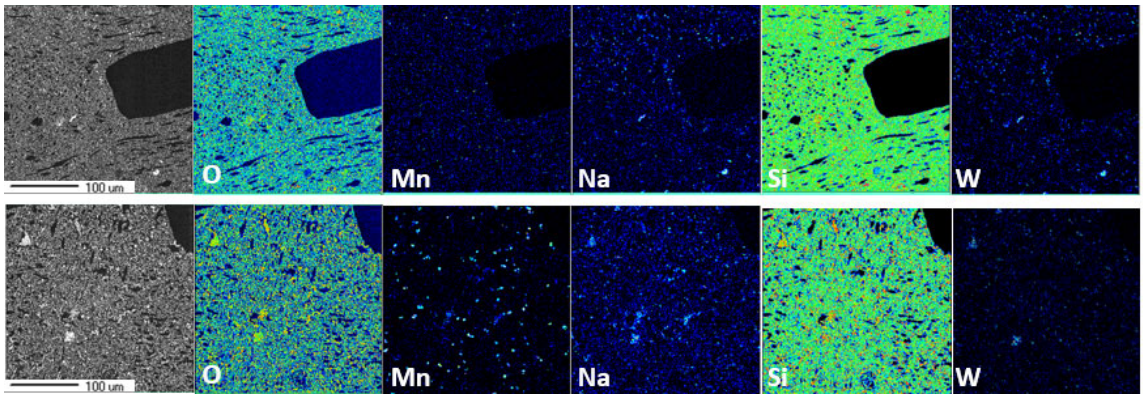

Figure S4. WDS images of 3D printed Mn-Na-W/SiO_2 catalyst before (top row) and after (bottom row) reaction showing elemental distribution and porosity as an effect of the exposure of the structure to the reaction conditions. Note that the catalyst material and pores are evenly distributed inside the structure.

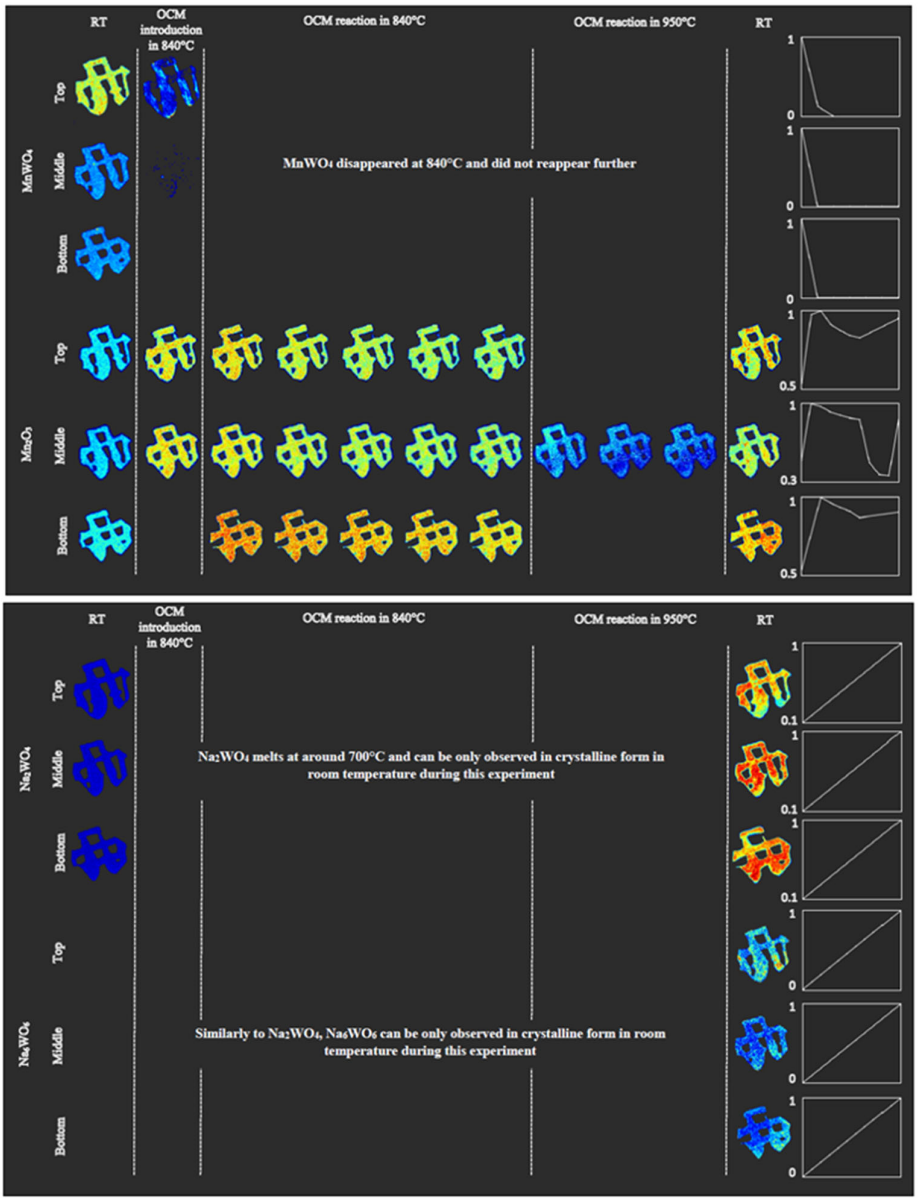

Figure S5. Phase distribution maps showing the evolution of each Mn- and Na-W oxide phase recorded across the silica support at three separate positions within the 3D printed sample. Mn_2O_3 was detected both at room temperature and at 840°C. $MnWO_4$ was recorded only at room temperature and did not reappear later during the measurement. Na_2WO_4 and Na_6WO_6 can be only observed in crystalline form at room temperature during this experiment.

The temperature dependent XRD measurements presented in Table S1 were performed on a PANalytical Empyrean, 60 kV with PIXcel^{3D}.

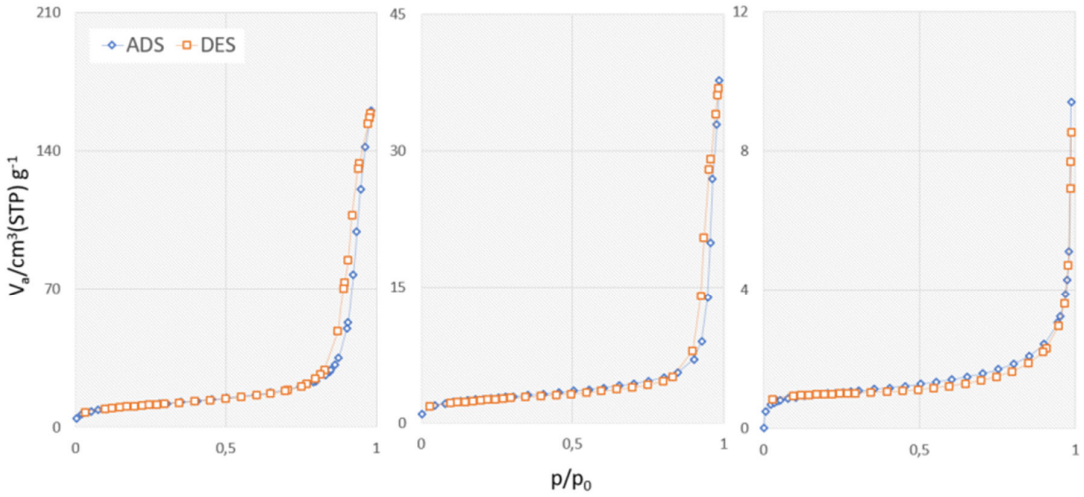

Abbildung 2.4: *Sorptionsisothermen der untersuchten Katalysatoren. Links: Pulver, Mitte: Struktur, Rechts: Pellet.*

Figure S6. N_2 adsorption-desorption isotherms for powder, 3D printed and pelletized Mn-Na-W-O/SiO_2 samples.

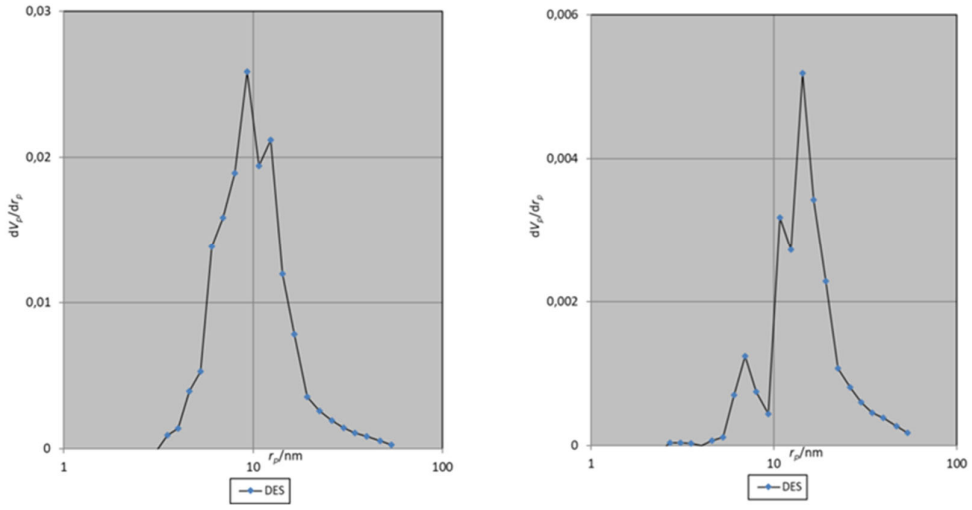

Figure S7. Pore diameter plots showing mesopore size distributions for the powder and 3D printed Mn-Na-W-O/SiO_2 samples.

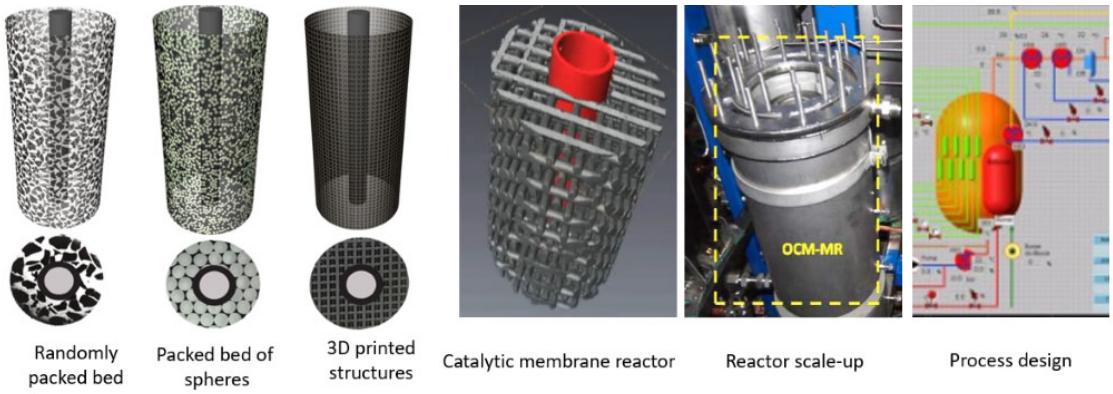

Figure S8. Scope for future work: from current fixed bed incarnations to catalytic membrane reactors comprising 3D printed monoliths and porous alumina membrane for O_2 distributive feed for a scaled up reactor design.

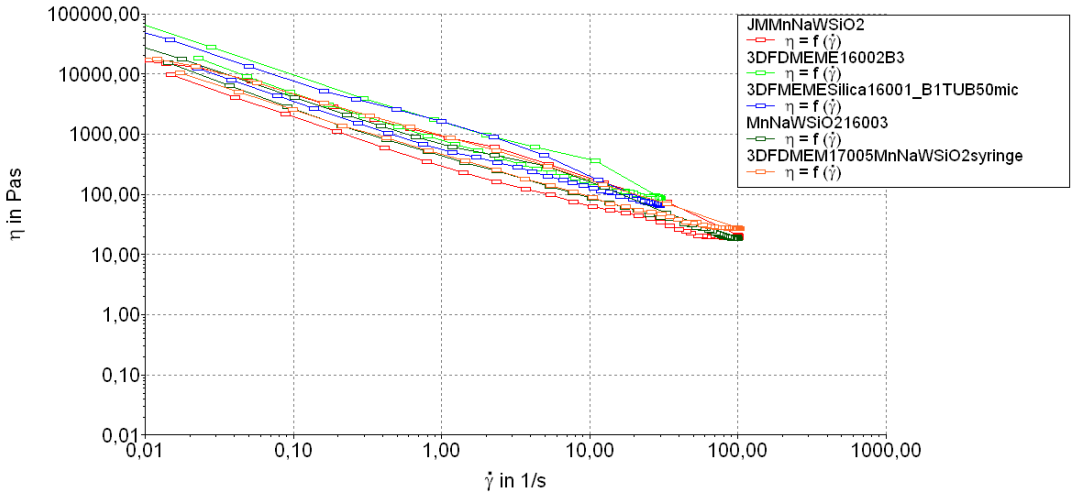

Figure S9. Viscosity (η) as a function of shear rate for typical MnNaW/SiO_2 printing pastes at 25 °C

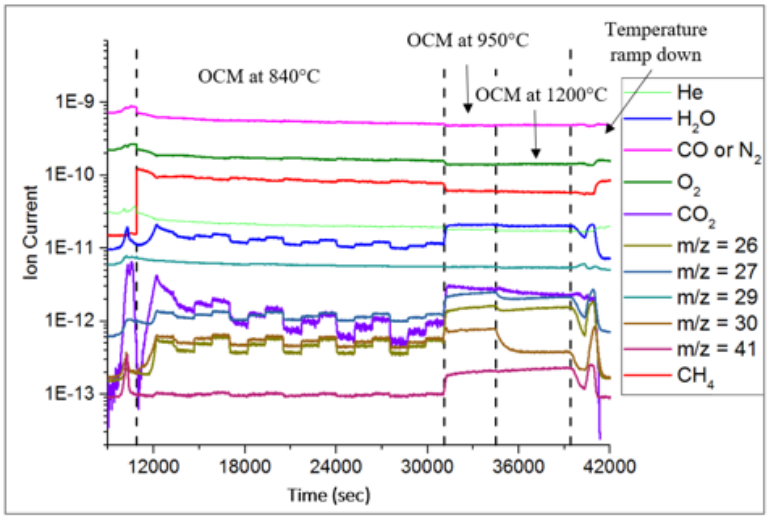

Figure S10. Mass spectrometry measurements under OCM at 840 °C for 5.5hrs during the in situ XRD-CT experiments

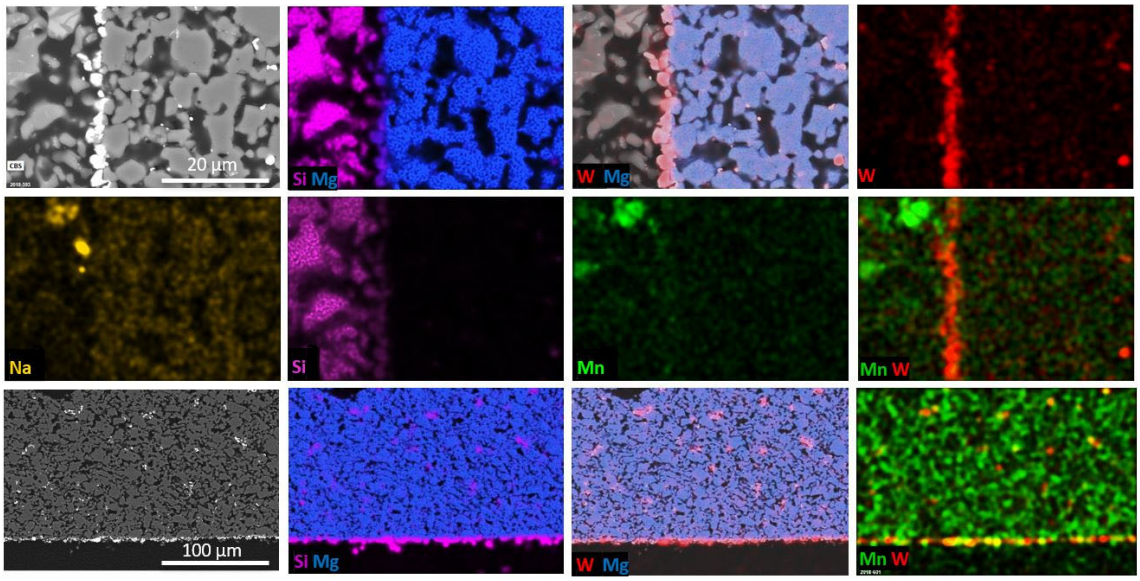

Figure S11. SEM and EDS images showing morphology and elemental mapping of spent Mn-Na-W/SiO_2 catalyst along the inner wall of a porous MgO membrane that was tested under OCM conditions at the ID15A beamline of the ESRF; (legend: Mn-green, W-red, Mg-blue, Si-fuchsia).

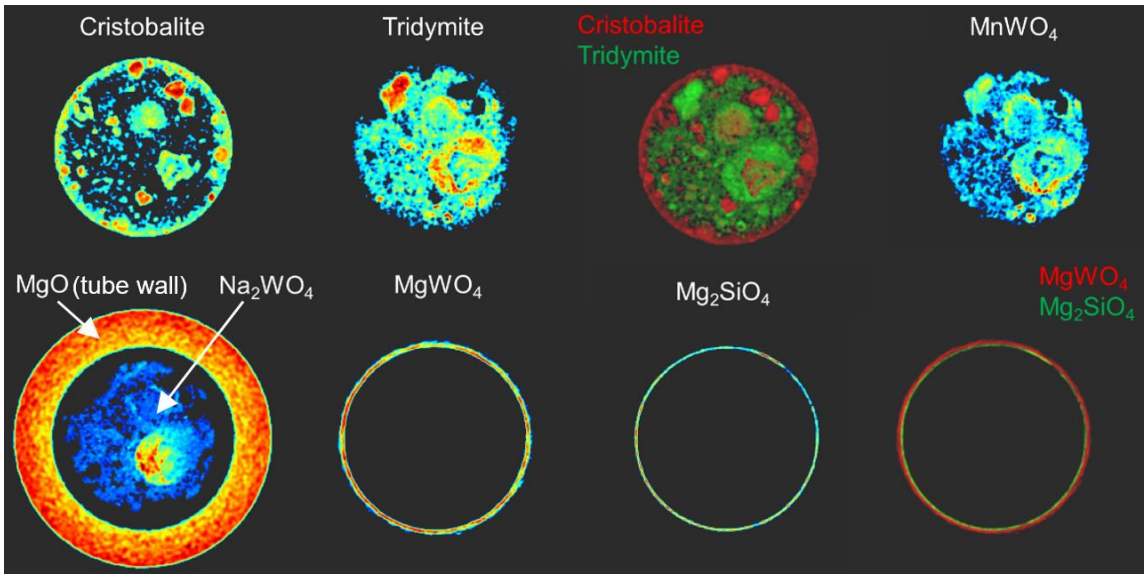

Figure S12. Phase distribution maps of cristobalite, tridymite, Na_2WO_4, $MnWO_4$, $MgWO_4$ and Mg_2SiO_4 at a selected height within a porous MgO membrane reactor after 40 h of operation. Note the formation of magnesium silicate on the wall of the MgO tubes and tungsten imbedding as a sublayer in the form of magnesium tungstate.

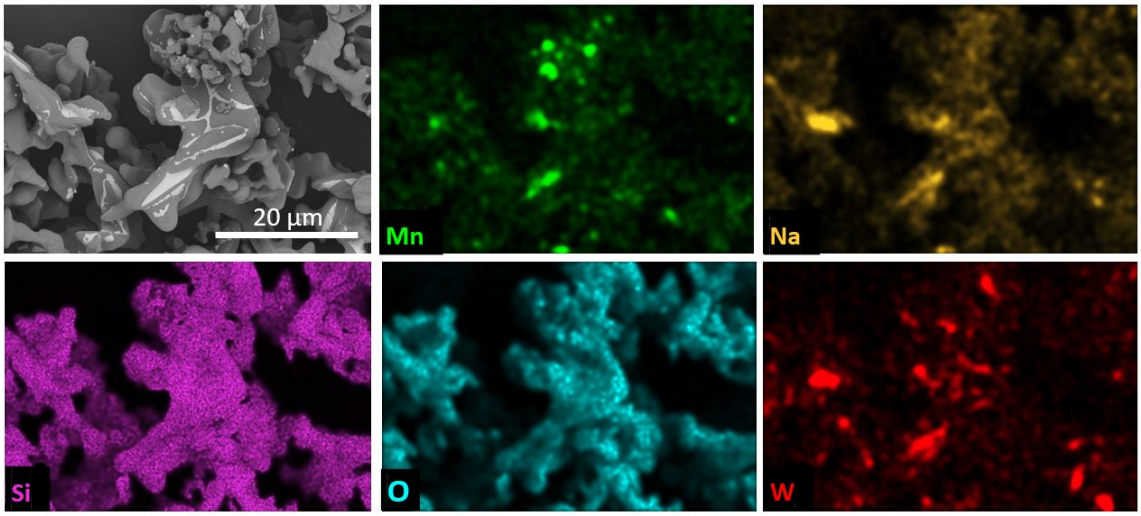

Figure S13. Representative elemental maps showing grains of the spent Mn-Na-W/SiO_2 catalyst in the pelletized powder form. Scale bar in all maps is 20 μm. Larger grains Mn (up to ca. 5 μm), and Na and W (up to ca.10 μm) were observed across the silica support.